



Granular transport through flighted rotary drums operated at optimum-loading: Mathematical model

Mohamed A. Karali, Eckehard Specht, Jochen Mellmann, H. A. Refaey, M. R. Salem & A. Y. Elbanhawy

To cite this article: Mohamed A. Karali, Eckehard Specht, Jochen Mellmann, H. A. Refaey, M. R. Salem & A. Y. Elbanhawy (2019): Granular transport through flighted rotary drums operated at optimum-loading: Mathematical model, *Drying Technology*, DOI: [10.1080/07373937.2019.1582062](https://doi.org/10.1080/07373937.2019.1582062)

To link to this article: <https://doi.org/10.1080/07373937.2019.1582062>



Published online: 07 Mar 2019.



Submit your article to this journal [↗](#)



View Crossmark data [↗](#)



Granular transport through flighted rotary drums operated at optimum-loading: Mathematical model

Mohamed A. Karali^a, Eckehard Specht^b, Jochen Mellmann^c, H. A. Refaey^d, M. R. Salem^d, and A. Y. Elbanhawey^e

^aDepartment of Mechanical Engineering, Faculty of Engineering and Technology, Future University in Egypt, New Cairo, Cairo, Egypt; ^bInstitute of Fluid Dynamics and Thermodynamics, Otto von Guericke University Magdeburg, Magdeburg, Universitätsplatz 2, Germany; ^cLeibniz Institute for Agricultural Engineering and Bioeconomy (ATB), Max-Eyth-Allee, Potsdam, Germany; ^dDepartment of Mechanical Engineering, Faculty of Engineering at Shoubra, Benha University, Cairo, Egypt; ^eDepartment of Mechanical Engineering, Faculty of Engineering, Ain Shams University, Cairo, Egypt

ABSTRACT

This paper discusses the transport of granular materials through flighted rotary drums operated at the optimum loading. A mathematical model is derived from the force balance acting on a single traveling particle, to predict the mean residence time of transportation. Based on the available parameters of mean height of falling curtains and final discharge angle, this model can be helpful to estimate the appropriate solid feeding rate. Two steps were followed to implement the use of the model. Firstly, experiments were carried out on a batch rotary drum to obtain the needed input parameters. Then, a case study of a small capacity rotary dryer was considered. In both steps, the drum was operated at the optimum loading. The model results were compared with other correlation from the literature for two cases of solid and air flows: con-current and counter current. Based on the results, a factor is introduced for generalized correlation from literature.

ARTICLE HISTORY

Received 5 July 2018
Revised 22 October 2018
Accepted 10 February 2019

KEYWORDS



Granular transport; rotary drums; rotary dryer; residence time; optimum loading

1. Introduction

Many basic products in our daily life including a variety of building materials, chemicals, pharmaceuticals and food are granular, such as sand, sugar, corn, wheat, salt, peanuts, flour, cement, limestone, fertilizers, wood chips, pills. A rotary drum is a popular device used in industry for the manufacturing and processing of many vital granular products. Rotary kilns, rotary dryers, and rotary coolers are the most commonly used types of rotary drums found in industry. A rotary drum consists of a long cylinder tilted to the horizontal and have the possibility to rotate around its axis. The solid granular is fed into the upper end of the drum by various methods including inclined chutes, overhung screw conveyors, and slurry pipes. The charge then travels down along the drum by axial and circumferential movements, due to the drum's inclination and rotation. During the traveling of the solid, it interacts with a processing gas along the drum specially in the so-called gas-borne area for a certain process. In either counter or co-current flow directions. Until the processed solid discharged from the

lower end of the drum.^[1–3] Rotary drum's interior wall is usually equipped with baffles known as lifters or flights, which helps for lifting the granular material from the bottom bed, then cascade, and showers it through the gas-borne area developing a series of curtains. Many flight configurations were developed to meet industrial requirements for a specific product. Blade or radial flight profile is used for sticky materials, while rectangular profile is mostly used for free-flowing bulk materials.^[4–6]

The loading of a flighted rotary drum highly influences the whole process.^[7] Three types of drum loading states can be categorized: under loading, optimum loading (or called design loading), and over loading which are characterized based on the holdup and the discharge angle of the first unloading flight (FUF).^[8] Detailed information of these loading types is found in Sunkara et al.^[9]: The optimum loading means the FUF starts to unload the material very close to the 9 o'clock position, while the unloading starts earlier before the 9 o'clock position in the over-loaded drum and lately than the 9 o'clock position in the case of under-loaded drum.

CONTACT Mohamed A. Karali  mkarali@fue.edu.eg  Department of Mechanical Engineering, Faculty of Engineering and Technology, Future University in Egypt, 90 St, New Cairo, Cairo, Egypt.

Color versions of one or more of the figures in the article can be found online at www.tandfonline.com/ldrt.

© 2019 Taylor & Francis Group, LLC

Many investigations from literature emphasize that the best performance of a flighted rotary drum occurs when the drum operates at the optimum loading conditions.^[10–11] Therefore, a lot of experimental and theoretical works have been carried out to assess the optimum loading of a flighted rotary drum. The determination criterion of the optimum loading was based on reaching saturation of the FUF by the solid material at the 9 o'clock position, while the experimental work depends on record videos in front of the drum. Then by means of different image processing and analysis methods, the area of the material reside in the flight can be obtained. Consequently, the volume and mass can be calculated.^[12]

The studying of the solid transport through a flighted rotary drum is of importance. As it helps to predict the mean time needed for the material processing (mean residence time), it consequently determines the feed rate at a specific drum loading. For example, in a rotary dryer, it is essential to predict the appropriate feeding rate as it shapes the quality of the product. Smaller residence time causes uneven drying of the feedstock, whereas higher residence time leads to over drying of the material which involves unaccepted changes in the product shape, properties, and moreover huge energy loss.^[1,13]

Transportation of solid through a flighted rotating drum is influenced by many parameters: the drum slope to the horizontal, the drum rotational speed, the lifting of the solid by the flights, the disperse nature into the gas stream, the bouncing in the gas and rolling, and the sliding of the particles on impact with the bottom of the dryer.^[14,15] Hence, the studying of the axial transport is much complicated, and a lot of assumptions for simplifications are needed.^[16,17]

For more understanding of the solid transport inside a flighted rotary drum, the physical description is introduced in the following section.

2. Physical description of granular solid transport in a flighted rotary drum

Figure 1 gives information about the motion behavior of granular solid in a flighted rotating drum. Considering a single particle of the solid transported through the drum, the particle is lifted up by the flight because of the rotation of the drum. From point A to point B see Figure 1(a,b) and then it is falling down from B to somewhere in the bottom (point C). After the particle has left the flight, it travels through the gas-borne area along the drum and subjected to drag force in a direction parallel to the axis of the

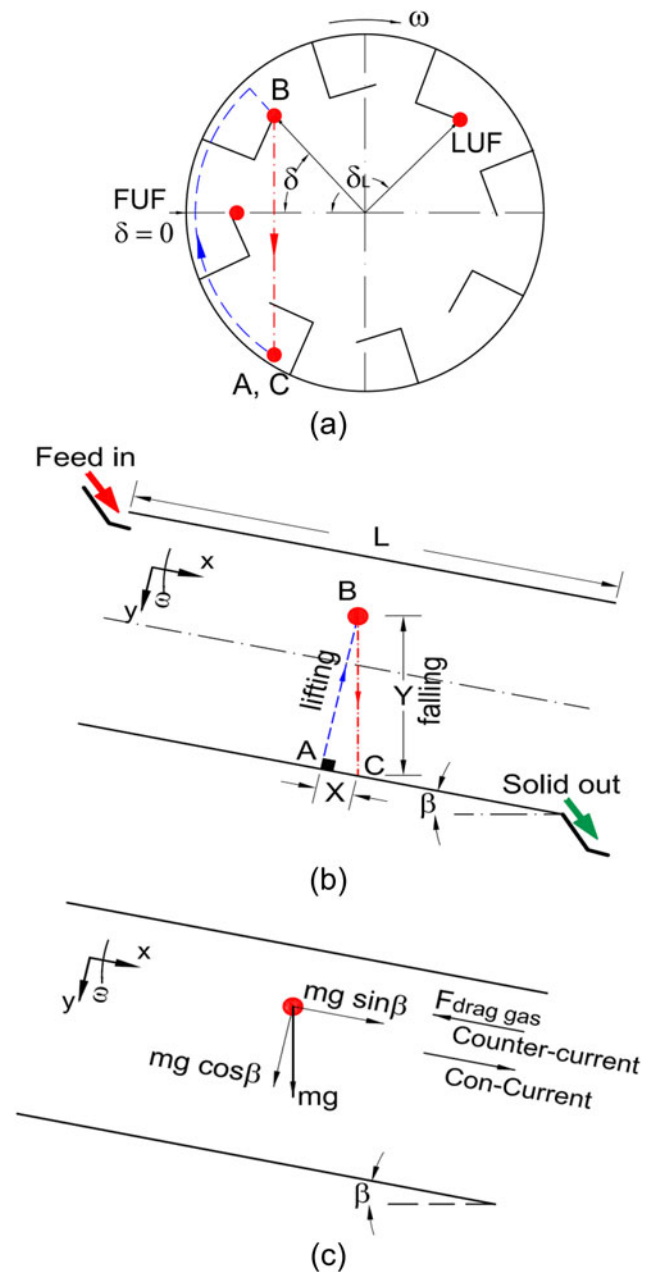


Figure 1. Falling of a particle in a flighted rotary drum inclined to the horizontal, (a) cross-sectional view, (b) axial view, (c) free body diagram showing external forces.

drum, and a drag force opposing the falling direction of the particle (see Figure 1(c)). The effect of the later is negligible compared to the accelerating force due to gravity. At the impact point at the bottom of the drum, the particle can be rolling and sliding until it begins another cascade cycle.^[18,19]

Because of the slope of the drum (β), a successful axial advance (X) by the particle is observed during the fall. And the particle motion forms a number of cascade cycles with an axial advance till it discharged from the drum. The number of cascades and the axial advance per cascade are determining the mean

residence time of the solid inside the drum. To determine the axial advance (X) by the particle, the equation of motion should be applied as will be described later.

It is worth noting that the first unloading flight (FUF) is at the nine o'clock position for the case of optimum loading drums ($\delta = 0$). The cascades of the particles are continuing until the last unloading flight (LUF) position ($\delta = \delta_L$).

Performing experiments on real flighted rotary drums to study the effect of many operating parameters on the mean residence time is difficult and costly. Instead, many solid transport mathematical models were developed and available in the literature, as discussed in the followings.

3. Models from literature

Many solid transport models of flighted rotary drums have involved the development of empirical relationships for the mean residence time (τ) from pilot-scale experiments.^[20,21] While simplistic in nature, pilot-scale empirical relationships generally lead to under prediction of measured values of the mean residence time in industrial rotary drums.^[22] An alternative technique was employed by researchers to determine the mean residence time using geometric models arguments based on the holdup of flights over the discharge angle.^[12] The mean residence time of solid in a rotary drum is influenced by four components of particle movement along the drum: a) gravitational force due to the slope of the drum, b) drag of the gas on the particles for counter-current flow, c) bouncing of the particles on impact with the bottom of the dryer, and d) rolling of the particles in the bed at the bottom of the drum, especially for over-loaded case. The last two components are almost impossible to predict theoretically and are therefore evaluated experimentally for each type of material as mentioned by Kemp and Oakley.^[23] Numerous equations have been proposed for the estimation of the mean residence time in rotary drums, and in the following are some models from literature.^[24–27]

In many of these studies, only average holdups and solid feed rate were considered.^[28] The mean residence time for the particles (τ) in these cases is given by

$$\tau = \frac{H_{\text{Tot}}}{\dot{m}_s} \quad (1)$$

where H_{Tot} is the total drum holdup in kg, usually determined by suddenly stopping the drum and

subsequently weighing its contents, and \dot{m}_s is the solid feed rate in kg/s.

One of the most frequently used empirical equation for residence time estimation was proposed by Friedman and Marshall^[11] and later modified by Foust et al.^[29]:

$$\tau = \frac{13.8L}{\tan(\beta)N^{0.9}D} \pm \frac{0.59L\dot{m}_a}{\sqrt{d_p}\dot{m}_s} \quad (2)$$

Here, the upper plus sign refers to the counter-current flow and the lower minus sign refers to the concurrent flow. β is the drum slope angle in degree, N is the rpm, L is the drum length in m, D is the drum diameter in m, and d_p is the particle diameter in m and \dot{m}_a and \dot{m}_s are in kg/s.

Saeman and Mitchell^[30] were the first to break away from the empirical approach to calculate rotary dryer holdups adopted by previous researchers. They analyzed material transport through the dryer in terms of incremental transport rates associated with individual cascade paths to yield a transport-rate distribution function. By assuming a linear relationship between the horizontal displacement of the particles due to the air flow and its velocity, they derived the following equation for the mean residence time:

$$\tau = \frac{L}{f(H)DN(\tan(\beta) \pm m'u_g)} \quad (3)$$

Where $f(H)$ is a cascade factor with values typically between 2 and π that increase as solids holdup increases, and m' is an empirical parameter (dimensional) for a given material. The positive sign in Equation indicates the con-current flow and the negative sign indicates the counter-current flow.

Schofield and Glikin^[31] derived the following residence time equation by considering the drag exerted by the air flowing counter-currently to the particles:

$$\tau = \frac{L}{y_{\text{avg}}\left(\sin(\beta) - \frac{ku_r^2}{g}\right)} \left[\left(\frac{2y_{\text{avg}}}{g}\right)^{0.5} + \frac{\delta_{\text{avg}}}{\pi N} \right] \quad (4)$$

where y_{avg} is the average falling height, u_r is the relative velocity between solid and gas, δ_{avg} is the average discharge angle corresponding to y_{avg} , and k is a factor for the drag force.

In other publications, the total residence time was calculated as the total number of cascades of a particle moving along the drum times the sum of the time of lifting and the time of falling per one cascade, where the number of cascades can be estimated based on the calculated axial advance of the particle per cascade. For such reason, a mathematical model was proposed by Kamke and Wilson.^[32] The axial advance of the

particle (X) per cascade was given by the following expression:

$$X = u_g t_{\text{fall}} + \frac{1}{k} \ln \left\{ \frac{\cos \left(\tan^{-1} (u_g/a_1) \right)}{\cos \left(-a_1 K t_{\text{fall}} + \tan^{-1} (u_g/a_1) \right)} \right\} \quad (5)$$

where a_1 and k are constants depending on the drum inclination and drag coefficient, respectively, u_g is the gas velocity, and t_{fall} is the falling time. The model has been validated with an experimental drum of 1.2 m in diameter and 5.5 m in length, with six centered flights and 12 flights installed to the outer shell of the dryer. The experiments were performed with wood particles having a sphericity of 0.75 and exposed to hot gas stream in con-current passion. The residence time was measured by injecting radioactive tracer particles at the inlet along with the feed. They noticed that within a curtain, the particles may be affected by the other particles and shielding of the gas flow can also occur. Due to this, the model over predicted the data collected, since the model assumes that the particles are independent to the gas flow. They noted that the particles may be attributed as a bulk material, and the mean diameter can be used in order to measure the drag coefficient. It has been found that the root-mean-square error was 109.6% in the case of discrete particle size, whereas, in case of mean diameter, it was around 14.2%.

Shahhosseini et al.^[33] proposed a steady-state semi-empirical model to predict solid holdup and flow rate in rotary dryers. Based on modifying the model of Friedman and Marshall,^[1] the dryer was modeled as a distributed parameter system. Experiments also have been done on a pilot scale rotary dryer for sugar. Results were used to investigate dynamics of the system in terms of solid motion and to validate the model.

Based on the analysis of a large amount of data found in the literature on the operation of rotary drums of many applications, on both pilot and industrial scales, Perry and Green^[34] proposed the following general correlation for calculation of the mean residence time:

$$\tau = \frac{KL}{\tan(\beta)N^{0.9}D} \quad (6)$$

Where K is a factor that depends on the number and format of the flights.

These models are mostly considering the case of over-loaded drums. In this paper, a mathematical model is derived for the solid transport inside a flighted rotary drum operated at optimum loading,

from the force balance acting on a single traveling particle, to predict the mean residence time of transportation. Based on available input parameters of mean height of falling curtains and final discharge angle at the optimum loading conditions, the approach advocated in this paper can be helpful to estimate the appropriate solid feeding rate.

4. Current work model description

4.1. Model assumptions

The following assumptions were accounted in the model:

- Steady state operation: with constant filling degree along the drum. This may be realistic, specially for the case of optimum-loading at no bed formation at the bottom of the drum. Hence, uniform discharge characteristics from the flights along the drum can be assumed.
- Neglect the interactions between particles (free flowing – non-cohesive). Each particle spent the same amount of time over the drum.
- The particle is of a spherical shape and it remains its dimensions and shape unchanged along the drum.
- Neglect the rotational effect on the particle after leaving the flight.
- Free and vertical fall of the particle (initially at zero velocity).
- Neglect the vertical drag force.
- No slip condition of the gas on the particle surface.
- Neglect transitional effects between the particle and the fluid.

4.2. Equationing

The free body diagram of the forces acting on a single particle falling freely from a flight in a rotary drum at a certain discharge angle (δ) and subjected to a gas flow (assumed air) is shown in Figure 1(c). Applying the equation of motion on the particle in the axial direction after considering the model assumptions^[35] reveals that

$$ma_x = \sum \text{Forces} \quad (7)$$

$$m \frac{du_x}{dt} = mg \sin(\beta) \mu k u_r^2 \quad (8)$$

$$\frac{du_x}{dt} = g \sin(\beta) \mu k u_r^2 \quad (9)$$

where the upper minus sign refers to air following

counter-current flows and the lower positive is for con-current. β is the drum inclination angle, u_r is the relative velocity between the particles, and the air can be calculated as

$$u_r = u_a \pm u_x \quad (10)$$

u_a is the air velocity, and u_x is the particle falling velocity component in x -direction. The upper positive sign refers to counter-current flows, and the lower minus sign is for the con-current.

u_x can be obtained by applying the free fall equation on the particle assuming the fall from rest and then by resolving the falling velocity u_y .

$$\frac{u_y^2}{2g} = y \quad (11)$$

$$u_x(y) = \frac{1}{2} \sqrt{2gy} \sin(\beta) \quad (12)$$

The calculated u_x is a function of the falling distance (y) which is already varying with the flight position (δ).

In order to simplify the solution, an average value of the falling distance can be considered and calculated by the integration of the measured falling height over the flight discharge angle as

$$y_{\text{avg}} = \bar{h}_{\text{fall}} = \frac{1}{\delta_L} \int_0^{\delta_L} h_{\text{fall}}(\delta) d\delta \quad (13)$$

where δ_L is the measured final discharge angle at a specific operating conditions, and thus, $u_{x,\text{avg}}$ can be obtained as

$$u_{x,\text{avg}} = \frac{1}{2} \sqrt{2gy_{\text{avg}}} \sin(\beta). \quad (14)$$

Then, the average relative velocity can be calculated for known air velocity as

$$u_{r,\text{avg}} = u_a \pm \frac{1}{2} \sqrt{2gy_{\text{avg}}} \sin(\beta) \quad (15)$$

Back to Equation (8), the term k (presented before in Equation (4)) can be calculated based on the drag coefficient C_D . The drag coefficient was evaluated using the commonly used Schiller–Naumann drag correlation^[18,32] as stated in the following:

$$k = 1.5 \frac{C_D \rho_a}{d_p \rho_p} \quad (16)$$

$$C_D = \frac{12}{\text{Re}} \quad \text{Re} < 0.2 \quad (17)$$

$$C_D = \frac{12(1 + 0.15\text{Re}^{0.687})}{\text{Re}} \quad 0.2 < \text{Re} \leq 1000 \quad (18)$$

$$C_D = 0.44 \quad \text{Re} > 1000 \quad (19)$$

$$\text{Re} = \frac{\rho_a u_{r,\text{avg}} d_p}{\mu_a} \quad (20)$$

where d_p is the particle diameter, ρ_p is the particle density, ρ_a is the fluid density, μ_a is the fluid dynamic viscosity, and Re is a modified Reynolds number calculated based on the relative velocity between the fluid and the particle.

The final solution of Equation (9) gives the axial advance of the particle per one cascade (lifting then falling) and it is found to be

$$X_{\text{avg}} = \frac{1}{2} (g \sin(\beta)) t_{\text{fall}(h,\text{avg})}^2 \mp \frac{1}{2} (k u_{r,\text{avg}}^2) t_{\text{fall}(h,\text{avg})}^2 \quad (21)$$

where $t_{\text{fall}(h,\text{avg})}$ is the average falling time calculated based on the calculated average falling height as

$$t_{\text{fall}(h,\text{avg})} = \sqrt{\frac{2\bar{h}_{\text{fall}}}{g}} \quad (22)$$

Then, the number of cascades can be drawn by dividing the total drum length by the axial advance per one cascade

$$C = \frac{L}{X} \quad (23)$$

During one cascade, the lifting time can be approximated as

$$t_{\text{lift,avg}} = \frac{2\delta_{\text{avg}}}{\omega} = \frac{\delta_{\text{avg}}}{\pi N} \quad (24)$$

where δ_{avg} is the discharge angle (in radians) corresponding to the calculated average height of fall,

$$\delta_{\text{avg}} = \delta(\bar{h}_{\text{fall}}). \quad (25)$$

ω is the angular velocity in rad/s, and N is the rotational speed in rps. Thus, the total average time elapsed by the particle in the drum (mean residence time τ in sec) can be estimated from the following relation:

$$\tau = C(t_{\text{lift,avg}} + t_{\text{fall}(h,\text{avg})}) \quad (26)$$

where $t_{\text{lift,avg}} + t_{\text{fall}(h,\text{avg})}$ is the total time per one cascade.

In order to calculate the total solid mass flow rate passing through the drum, a new average solid velocity should be introduced where the subscript (s) denotes the solid material as

$$u_{\text{avg},s} = \frac{L}{\tau} \quad (27)$$

The total drum holdup H_{Tot} in $\text{m}^3/\text{m} = \text{m}^2$ can be estimated using the following relation:

$$H_{\text{Tot}} = f_{\text{optimum}} \cdot \pi R^2. \quad (28)$$

The optimum loading filling degree (f_{optimum}) could be estimated using correlations from the literature.^[12]

By multiplying the total drum holdup H_{Tot} with the real drum length, the total solid volume (m^3) could be obtained,

$$V_s = H_{\text{Tot}}L \quad (29)$$

hence the mass of solid (in kg) can be calculated using the solid bulk density (ρ_b) as

$$m_s = \rho_b V_s. \quad (30)$$

Finally, the needed solid mass flow rate can be calculated either by dividing the solid mass (m_s) by the total residence time (τ) or by using the calculated solid average velocity, total holdup, and the solid bulk density as

$$\dot{m}_s = \rho_b H_{\text{Tot}} u_{\text{avg},s}. \quad (31)$$

To implement the use of the model, two steps were followed. Experiments were carried out on a batch rotary drum, to obtain needed input parameters for the model: mean height of falling curtains and final discharge angle, at a specific operating conditions. Then, a case study of a small capacity rotary dryer was considered. In both steps, the drum was operated at the optimum loading.

5. Methods and materials

5.1. Test rig

Figure 2 shows the experimental apparatus. The test rig consists of a 0.5-m-internal-diameter and 15-cm-length rotating drum. The drum was directly coupled with an electrical motor and rotated in the clockwise direction. The rotating speed of the motor was controlled by a variable frequency inverter. The drum was set up with zero inclination with respect to the horizontal position on the ground in all directions. In order to maintain uniform solid distribution inside the drum, a line was stretched horizontally in front of the drum and was located at the center point level of the drum. This line acts as the reference demarcation of the 9 o'clock position. A total of 12 rectangular flights are installed at the inner drum surface with same radial length ($l_1=5$ cm) and tangential length (l_2) of 3.75 cm forming a flight tangential to radial length ratio $l_2/l_1=0.75$.

The drum's front side was covered with a circular glass plate and the rear end with a metal wall. In front of the drum, a high definition video camera had been placed perpendicularly to the plane of the glass plate.

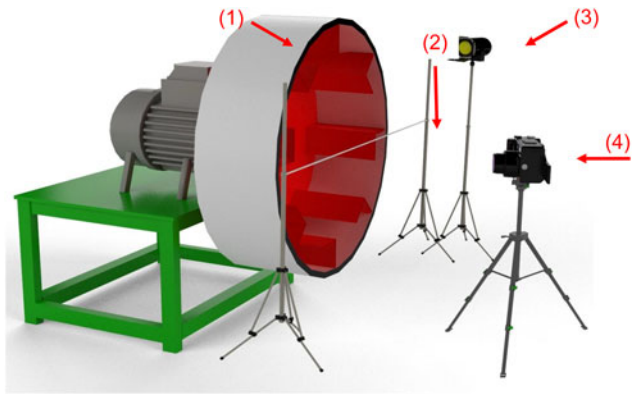


Figure 2. Experimental test rig; (1) experimental drum coupled with an electrical motor, (2) horizontal demarcation line, (3) light, and (4) digital FHD camera.

Table 1. Specifications of drum and operating parameters.

Drum diameter D	0.5 m
Drum length L	0.15 m
Flight length ratio l_2/l_1	0.75
Number of flights n_f	12
Rotational Speed rpm	3 rpm

A Canon 60 D still camera was used with attached 18–125 mm focal length lens. The video recording was set with auto-exposure, and the video quality was set with 1920×1080 pixels and 24 frames per second. The available shortest focal length of lens was adjusted to 18 mm for a wider angle of view. The focal point was focused at the center point of the drum to reduce the video distortion effects and parallax error during the recording of the entire drum object.

For the consistency of light exposure, the experiments were performed in a dark room and a light source was placed and directed toward the drum. The position of the light was carefully placed to avoid the reflection of light at the surface of glass which would lead to glaring of the video. Also, the light was distributed equally over the whole drum to facilitate the manual image analysis and to reduce eye strain.

5.2. Experimental procedures

The experimental procedure after the preparation of experimental setup was as follows: The amount of solid was determined in terms of the needed filling degree to achieve optimum loading of the drum using our correlation found in Karali et al.^[12] After the drum was fed with the solid, it was allowed to rotate until the desired rpm and then checked for optimum loading by reaching the saturation of the FUF and starting the first unloading at the 9 o'clock position. After some time and reaching steady operation, photographs were captured by the camera. The

Table 2. Physical properties of material to be tested.

Material	d_p (mm)	ρ_b (consolidated) (kg/m ³)
Glass beads	1.0	1555 ± 22

photographs were analyzed manually using ImageJ software^[35–38] to measure the followings: a) the final discharge angle (δ_L) and b) the height of falling curtains ($h_{fall(\delta)}$).

5.3. Operating parameters

Table 1 summarizes the drum specifications and operating parameters. Table 2 gives information about the granular material used.

5.4. Experimental results

Cascading of solid from flights forms a number of falling curtains equal to the number of active flights. The height of a falling curtain can be measured directly from photographs as the vertical distance of a particle leaving a flight tip to the first strike point at the bottom of drum. This height of fall determines the time the particles will stay in the gas-borne phase where they are exposed to the gas stream. The strike point differs according to the filling degree of the drum. For example, for an over-loaded drum, most of strike points are found to be on the bottom solid bed surface, while for the case of optimum-loaded drum, the bottom solid bed is no longer exists (see Figure 1). However, in some cases, the impact point is

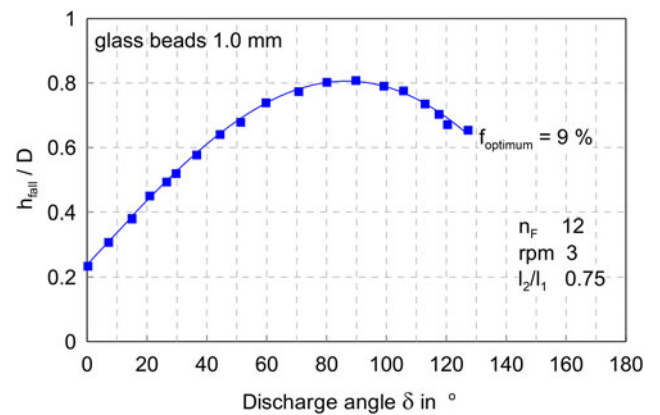


Figure 3. Measured curtains falling height of a single flight against flight tip angle. In a flighted rotary drum operated at optimum loading (12 flights, 0.75 flight length ratio, 3 rpm) and using glass beads (1 mm).

(1 mm) are at 0.75 flight length ratio, 3 rpm, and 12 flights. The measured height of falling curtains is represented as a dimensionless quantity divided by drum diameter. The final discharge angle can be found from the graph 3 to be 128°.

6. Case study

6.1. Given data

The mathematical model described previously is applied on a small capacity rotary dryer operated at optimum loading, with the following specifications:

Drum dimensions:	$D = 0.5$ m (taken exactly as the current work test rig), $L = 2.5$ m ($L/D = 5$ ^[32,33]), Filling degree = $f_{optimum} = 9\%$, $N = 3$ rpm (0.05 rps), $\omega = 0.314$ rad/s, $n_F = 12$, $l_2/l_1 = 0.75$, Drum slope (β) = 4° (0.0697 rad).
Solid properties:	glass beads, $d_p = 1.0$ mm, $\rho_p = 2650$ kg/m ³ , $\rho_b = 1555$ kg/m ³ .
Fluid properties:	Air at 115 °C, properties from Incropera and Dewitt, ^[39] $\rho_a = 0.8711$ kg/m ³ , $\mu_a = 0.000023$ Pa.s, $u_a =$ varied from 0.2 to 0.5 m/s.
Required:	Calculate for the two cases: counter-current and con-current and for the mentioned range of air velocity, the followings are average axial advance per one cascade, mean residence time, and average solid mass flow rate at optimum loading conditions.

located at the metal back side of the down opposite flight. As a conclusion, maximum falling height can be achieved when operating the drum at the optimum loading filling degree. Figure 3 depicts the variation of measured height of falling curtains along with flight tip angle. From the FUF position ($\delta=0$) to the LUF ($\delta=\delta_L$), at optimum loading conditions, glass beads

6.2. Case study results

Figure 4 represents the variation of the axial advance per one cascade of a falling particle at the different air velocities for two types of flows: counter-current and con-current. It is obviously shown in Figure 4 that the average axial advance of the counter-current flow type

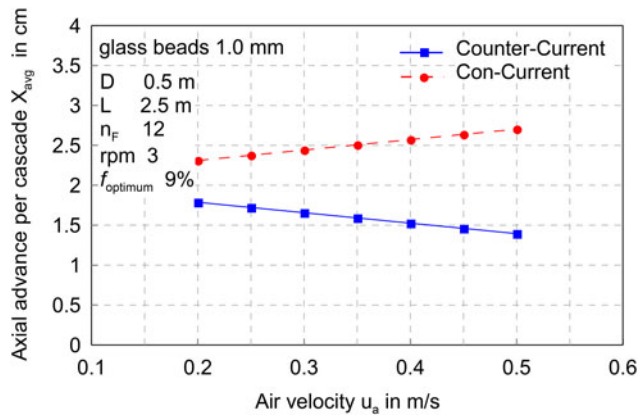


Figure 4. Variation of the axial advance per one cascade of falling particle with the air velocity for two types of air flows counter-current and con-current.

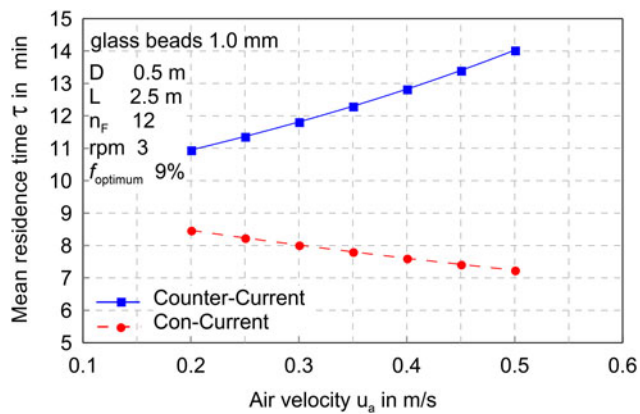


Figure 5. Variation of the mean residence time with the air velocity for two types of flows counter-current and con-current.

is lower than the one of the con-current flow types. This is mainly attributed to the higher drag coefficient (k) achieved by the counter-current flow. From Figure 4, it can be seen that increasing the air flow rate causes a decrease in the axial advance for the case of counter-current flow where the air is resisting the particle advance, while for the case of con-current flow, the axial advance increases as the air flow rate increases.

Figure 5 illustrates the variation of the predicted mean residence time against different air velocities for two types of flows: counter-current and con-current. It is shown in Figure 5 that the mean residence time elapsed by the solid in the drum for the counter-current flow type is higher than the one of the con-current flow types. From Figure 5, it can be seen that increasing the air flow velocity causes the mean residence time to increase for the case of counter-current flow type as the drag force increased, while for the

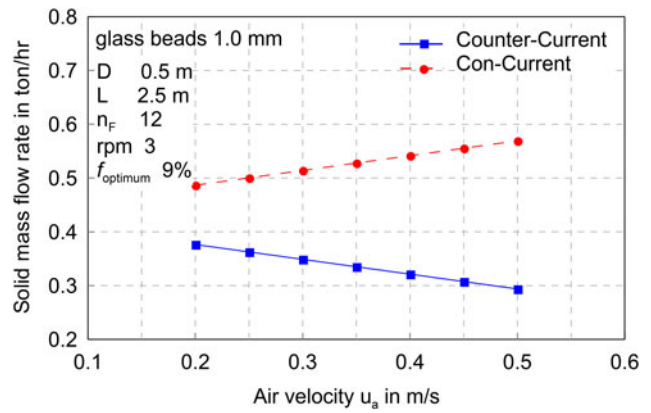


Figure 6. Variation of the solid mass flow rate with the air velocity for two types of flows counter-current and con-current.

case of con-current flow type, the mean residence time decreases as the air flow velocity increases as the drag force decreases.

Figure 6 depicts the variation of the solid flow rate with the air velocity for two types of flows: counter-current and con-current. It is clear from Figure 6 that the average solid flow rate for the counter-current flow type is lower than the one of the con-current flows. This is mainly because of the higher residence time needed for the counter-current flow type. Figure 6 shows that increasing the air flow rate causes a decrease in the solid flow rate for the case of counter-current flow type, While for the case of con-current flow type, the solid flow rate increases as the air flow rate increases.

The model results of the mean residence time are compared with the commonly used correlation from the literature. Correlation of Friedman and Marshall^[1] and later modified by Foust et al.^[29] described previously by Equation (2). The comparison is tabulated in Table 3 and shows high deviations between the two results. Similar deviation was reported by previous studies: Iguaz et al.^[40] and Abbasfard et al.^[41,42] That indicates it is of importance to carry out more experiments on real scale drums to investigate the time taken by the solid at different operating conditions.

The results from this work of the mean residence time are substituted in the general model of Perry and Green^[34] (Equation (6)) along with the corresponding values of operating parameters, resulting in an average value for the factor K of 22.7 as shown in Equation (32). It worth noting that, this is valid for the case of a drum equipped with 12 rectangular flights of 0.75 flight tangential to radial length ratio. Where, τ is in seconds, L and D are in meters, β is in degrees, and N is in rpm.

Table 3. Comparison of residence time with correlation from literature.

v_a in m/s	τ in min					
	Counter-current flow			Con-current flow		
	Current model, Equation (26)	Foust et al. ^[27]	deviation %	Current model, Equation (26)	Foust et al. ^[27]	deviation %
0.20	10.94	6.38	-41.67	8.46	5.85	-30.84
0.25	11.36	6.46	-43.11	8.23	5.77	-29.83
0.30	11.81	6.55	-44.55	8.01	5.69	-28.96
0.35	12.29	6.64	-45.99	7.80	5.60	-28.24
0.40	12.82	6.74	-47.43	7.60	5.50	-27.68
0.45	13.39	6.85	-48.88	7.41	5.39	-27.30
0.50	14.02	6.96	-50.32	7.23	5.27	-27.15

$$\tau = \frac{22.7L}{\tan(\beta)N^{0.9}D} \quad (32)$$

7. Conclusion

A simple mathematical model is derived from the force balance acting on a traveling particle through a flighted rotating drum. To predict the mean residence time of transportation. Experiments were performed on a batch rotary drum, to get needed input parameters for the model: mean height of falling curtains and final discharge angle, at a specific operating conditions. The drum was of 0.5 m diameter, available with 0.15 m length, and rotates at 3 rpm, having 12 flights of 0.75 flight tangential to radial length ratio. A case study of a small capacity rotary dryer of $D=0.5$ m and $L=2.5$ m was considered in order to test the model. For both the experiments and the case study, the drum was operated at the optimum loading. The model results were compared with the correlation of Foust et al.,^[29] for two cases of solid and air flows: con-current and counter current. The results revealed high deviation between the current work model and the model of Foust et al.^[29] Similar deviation was reported by other researchers, indicating that it is of importance to carry out more experiments on real scale drums to investigate the time taken by the solid at different operating conditions. Based on the results, a factor K with average value of 22.7 is introduced to be substituted in the general model of Perry and Green.^[34]

Nomenclature

A, B, C	points shown in Figure 1
C	the number of cascades
C_D	drag coefficient
D	drum diameter (m)
d_p	particle diameter (m)
f	filling degree (%)
FUF	first unloading flight
g	gravitational acceleration (m/s^2)

h	curtains height of fall (m)
H	holdup (m^3/m or cm^2)
K	fitting parameter in Equation (6)
L	drum length (m)
l_1	flight radial length (m)
l_2	flight tangential length (m)
LUF	last unloading flight
m	mass (kg)
\dot{m}	mass flow rate (kg/sec)
N	rotational speed (rpm)
n_F	total number of flights
Re	Reynolds number
t	time (sec)
u	velocity
V	volume (m^3)
X	Axial advance (cm)
x, y	direction axes

Greek letters

β	drum slope angle (o)
τ	mean residence time (sec)
δ	flight tip angle (°)
μ	viscosity (Pa.s)
ρ_a	air density (kg/m^3)
ρ_b	solid bulk density (consolidated) (kg/m^3)
ρ_p	solid particle density (kg/m^3)
ω	Drum angular velocity (rad/s)

Subscripts

a	air
avg	average
b	solid bulk
F	flight
L	final discharge angle optimum optimum loading
p	particle
r	relative
Tot	total

References

- [1] Friedman, S. J. Marshall, W. R. Studies in Rotary Drying: Part 1 – Holdup and Dusting. *Chem. Eng. Prog.* **1949**, 45, 482–573.
- [2] Mujumdar, A. S. Principles, classification, and selection of dryers. In *Handbook of industrial drying*, 3rd ed., Mujumdar, A. S., ed.; Taylor & Francis Group, **2007**, pp 4–31.

- [3] Karali, M. A. Analysis Study of the Axial Transport and Heat Transfer of a Flighted Rotary Drum operated at Optimum Loading. Ph.D. Dissertation, Otto-von-GuerickeUniversity Magdeburg, Germany, **2015**.
- [4] Kelly, J. J. Flight Design in Rotary Dryers. *Drying Technol.* **1992**, *10*, 979–993. DOI: [10.1080/07373939208916491](https://doi.org/10.1080/07373939208916491).
- [5] Baker, C. G. J. The Design of Flights in Cascading Rotary Dryers. *Drying Technol.* **1988**, *6*, 631–653. DOI: [10.1080/07373938808916402](https://doi.org/10.1080/07373938808916402).
- [6] Revol, D.; Briens, C. L.; Chabagno, J. M. The Design of Flights in Rotary Dryers. *Powder Technol.* **2001**, *121*, 3, 230–238. DOI: [10.1016/S0032-5910\(01\)00362-X](https://doi.org/10.1016/S0032-5910(01)00362-X).
- [7] Nascimento, S. M.; Duarte, C. R.; Barrozo, M. A. S. Analysis of the Design Loading in a Flighted Rotating Drum Using High Rotational Speeds. *Drying Technol.* **2018**, *36*, 1200–1208. DOI: [10.1080/07373937.2017.1392972](https://doi.org/10.1080/07373937.2017.1392972).
- [8] Ajayi, O. O.; Sheehan, M. E. Application of Image Analysis to Determine Design Loading in Flighted Rotary Dryers. *Powder Technol.* **2012**, *223*, 123–130. DOI: [10.1016/j.powtec.2011.05.013](https://doi.org/10.1016/j.powtec.2011.05.013).
- [9] Sunkara, K. R.; Herz, F.; Specht, E.; Mellmann, J.; Erpelding, R. Modeling the Discharge Characteristics of Rectangular Flights in a Flighted Rotary Drum. *Powder Technol.* **2013**, *234*, 107–116. DOI: [10.1016/j.powtec.2012.09.007](https://doi.org/10.1016/j.powtec.2012.09.007).
- [10] Sheehan, M. E.; Britton, P.; Schneider, P. A Model for Solids Transport in Flighted Rotary Dryers Based on Physical Considerations. *Chem. Eng. Sci.* **2005**, *60*, 4171–4182. DOI: [10.1016/j.ces.2005.02.055](https://doi.org/10.1016/j.ces.2005.02.055).
- [11] Sunkara, K. R.; Herz, F.; Specht, E.; Mellmann, J. Influence of Flight Design on the Particle Distribution of a Flighted Rotating Drum. *Chem. Eng. Sci.* **2013**, *90*, 101–109. DOI: [10.1016/j.ces.2012.12.035](https://doi.org/10.1016/j.ces.2012.12.035).
- [12] Karali, M. A.; Sunkara, K. R.; Herz, F.; Specht, E. Experimental Analysis of a Flighted Rotary Drum to Assess the Optimum Loading. *Chem. Eng. Sci.* **2015**, *138*, 772–779. DOI: [10.1016/j.ces.2015.09.004](https://doi.org/10.1016/j.ces.2015.09.004).
- [13] Tarhan, S.; Telci, İ.; Tuncay, M. T.; Polatci, H. Product Quality and Energy Consumption When Drying Peppermint by Rotary Drum Dryer. *Ind. Crops Prod.* **2010**, *32*, 420–427. DOI: [10.1016/j.indcrop.2010.06.003](https://doi.org/10.1016/j.indcrop.2010.06.003).
- [14] Britton, P.; Sheehan, M. E.; Schneider, P. A Physical Description of Solids Transport in Flighted Rotary Dryers. *Powder Technol.* **2006**, *165*, 153–160. DOI: [10.1016/j.powtec.2006.04.006](https://doi.org/10.1016/j.powtec.2006.04.006).
- [15] Rojas, R.; Piña, J.; Bucalá, V. ; Solids Transport Modeling in a Fluidized Drum Granulator. *Ind. Eng. Chem. Res.* **2010**, *49*, 6986–6997. DOI: [10.1021/ie901691v](https://doi.org/10.1021/ie901691v).
- [16] Duchesne, C.; Thibault, J.; Bazin, C. Modeling of the Solids Transportation within an Industrial Rotary Dryer: A Simple Model. *Ind. Eng. Chem. Res.* **1996**, *35*, 2334–2341. DOI: [10.1021/ie950625j](https://doi.org/10.1021/ie950625j).
- [17] Renaud, M.; Thibault, J.; Trusiak, A. Solids Transportation Model of an Industrial Rotary Dryer. *Drying Technol.* **2000**, *18*, 843–865. DOI: [10.1080/07373930008917741](https://doi.org/10.1080/07373930008917741).
- [18] Glikin, P. G. Transport of Solids through Flighted Rotating Drums. *Trans. Inst. Chem. Eng.* **1978**, *56*, 120–126.
- [19] Cronin, K.; Catak, M.; Bour, J.; Collins, A.; Smee, J. Stochastic Modelling of Particle Motion along a Rotary Drum. *Powder Technol.* **2011**, *213*, 79–91. DOI: [10.1016/j.powtec.2011.07.009](https://doi.org/10.1016/j.powtec.2011.07.009).
- [20] Sai, P. S. T. Drying of Solids in a Rotary Dryer. *Drying Technol.* **2013**, *31*, 213–223. DOI: [10.1080/07373937.2012.711406](https://doi.org/10.1080/07373937.2012.711406).
- [21] Delele, M. A.; Weigler, F.; Mellmann, J. Advances in the Application of a Rotary Dryer for Drying of Agricultural Products: A Review. *Drying Technol.* **2015**, *33*, 541–558. DOI: [10.1080/07373937.2014.958498](https://doi.org/10.1080/07373937.2014.958498).
- [22] Cao, W. F.; Langrish, T. A. G. Comparison of Residence Time Models for Cascading Rotary Dryers. *Drying Technol.* **1999**, *17*, 825–836. DOI: [10.1080/07373939908917572](https://doi.org/10.1080/07373939908917572).
- [23] Kemp, I. C.; Oakley, D. E. Simulation and Scale-up of Pneumatic Conveying and Cascading Rotary Dryers. *Drying Technol.* **1997**, *15*, 1699–1710. DOI: [10.1080/07373939708917319](https://doi.org/10.1080/07373939708917319).
- [24] Austin, L. G.; Shoji, K.; Hogg, R.; Carlson, J.; Flemmer, R. L. C. Flow Rates of Dry Powders in Inclined Rotating Cylinders under Open Ended Discharge Conditions. *Powder Technol.* **1978**, *20*, 219–225. DOI: [10.1016/0032-5910\(78\)80052-7](https://doi.org/10.1016/0032-5910(78)80052-7).
- [25] Alvarez, P. I.; Shene, C. Experimental Study of Residence Time in a Direct Rotary Dryer. *Drying Technol.* **1994**, *12*, 1629–1651. DOI: [10.1080/07373939408962190](https://doi.org/10.1080/07373939408962190).
- [26] Lisboa, M. H.; Vitorino, D. S.; Delaiba, W. B.; Finzer, J. R. D.; Barrozo, M. A. S. A Study of Particle Motion in Rotary Dryer. *Braz. J. Chem. Eng.* **2007**, *24*, 365–374. DOI: [10.1590/S0104-66322007000300006](https://doi.org/10.1590/S0104-66322007000300006).
- [27] Thibault, J.; Alvarez, P. I.; Blasco, R. ; Vega, R. Modelling the Mean Residence Time in a Rotary Dryer for Various Types of Solids. *Drying Technol.* **2010**, *28*, 1136–1141. DOI: [10.1080/07373937.2010.483045](https://doi.org/10.1080/07373937.2010.483045).
- [28] Kelly, J. J.; O'Donnell, J. P. Residence Time Model for Rotary Drums. *Trans. IChemE.* **1977**, *55*, 243–252.
- [29] Foust, A. S.; Wenzel, L. A.; Clump, C. W.; Maus, L.; Andersen, L. B. *Principles of Unit Operations*; Wiley: New York, **1960**.
- [30] Saeman, W. C.; Mitchell, T. R. Analysis of Rotary Dryer a Cooler Performance. *Chem. Eng. Prog.* **1954**, *50*, 467–475.
- [31] Schofield, F. R.; Glikin, P. G. Rotary Coolers for Granular Fertilizer. *Chem. Process Eng. Resour.* **1962**, *40*, 183.
- [32] Kamke, F. A.; Wilson, J. B. Computer Simulation of a Rotary Dryer. Part II: Heat and Mass Transfer. *Am. Inst. Chem. Eng.* **1986**, *32*, 269–275. DOI: [10.1002/aic.690320214](https://doi.org/10.1002/aic.690320214).
- [33] Shahhosseini, S.; Cameron, I. T.; Wang, F. A Simple Dynamic model for Solid Transport in Rotary Dryers. *Drying Technol.* **2000**, *18*, 867–886. DOI: [10.1080/07373930008917742](https://doi.org/10.1080/07373930008917742).

- [34] Perry, R. H.; Green, D. W. *Chemical Engineers Handbook*; McGraw – Hill: New York, **1999**.
- [35] Maxey, M. R.; Riley, J. Equation of Motion for a Small Rigid Sphere in a Turbulent Fluid Flow. *Phys. Fluids*. **1983**, *26*, 883–889. DOI: [10.1063/1.864230](https://doi.org/10.1063/1.864230).
- [36] Karali, M. A.; Herz, F.; Specht, E.; Mallmann, J. Comparison of Image Analysis Methods to Determine the Optimum Loading of Flighted Rotary Drums. *Powder Technol.* **2016**, *291*, 147–153. DOI: [10.1016/j.powtec.2015.11.053](https://doi.org/10.1016/j.powtec.2015.11.053).
- [37] Karali, M. A.; Herz, F.; Specht, E.; Mellmann, J. Different Camera and Light Positions to Facilitate Image Analysis Processing in Rotary Drums Studies. *Powder Technol.* **2017**, *306*, 55–60. DOI: [10.1016/j.powtec.2016.10.013](https://doi.org/10.1016/j.powtec.2016.10.013).
- [38] Karali, M. A.; Herz, F.; Specht, E.; Mellmann, J.; Refaey, H. A. Unloading Characteristics of Flights in a Flighted Rotary Drum Operated at Optimum Loading. *Powder Technol.* **2018**, *333*, 347–352. DOI: [10.1016/j.powtec.2018.04.052](https://doi.org/10.1016/j.powtec.2018.04.052).
- [39] Incropera, F. P.; Dewitt, D. P.; Bergman, T. L.; Lavine, A. S. *Fundamental of Heat and Mass Transfer*. John Wiley & Sons, Inc: New York, **2007**.
- [40] Iguaz, A.; Esnoz, A.; Martínez, G.; López, A.; Vírveda, P. Mathematical Modeling and Simulation for the Drying Process of Vegetable Wholesale By-products in a Rotary Dryer. *J. Food Eng.* **2003**, *59*, 151–160. DOI: [10.1016/S0260-8774\(02\)00451-X](https://doi.org/10.1016/S0260-8774(02)00451-X).
- [41] Abbasfard, H.; Rafsanjani, H. H.; Ghader, S.; Ghanbari, M. Mathematical Modeling and Simulation of an Industrial Rotary Dryer: A Case Study of Ammonium Nitrate Plant. *Powder Technol.* **2013**, *239*, 499–505. DOI: [10.1016/j.powtec.2013.02.037](https://doi.org/10.1016/j.powtec.2013.02.037).
- [42] Abbasfard, H.; Ghader, S.; Rafsanjani, H. H.; Ghanbari, M. Mathematical Modeling and Simulation of Drying Using Two Industrial Concurrent and Countercurrent Rotary Dryers for Ammonium Nitrate. *Drying Technol* **2013**, *31*, 1297–1306. DOI: [10.1080/07373937.2013.791307](https://doi.org/10.1080/07373937.2013.791307).